Sol-gel synthesis of zirconia-based nanoparticles from the side product of tin mining

Anis Kristiani[1], Wiyono[2], *Arif* Prasetiyo[2], *Himawan Tri Bayu Murti* Petrus[3,4], *Siti Nurul Aisyiyah* Jenie[1], Adid *Adep* Dwiatmoko[1], *Luthfiana Nurul* Hidayati[1], *Fauzan* Aulia[1], Sudiyarmanto[1], and *Deliana* Dahnum[1]

[1]Research Centre for Chemistry, National Research and Innovation Agency (BRIN) Building 452 Kawasan Sains dan Teknologi BJ. Habibie Serpong, Tangerang Selatan, 15314, Banten, Indonesia
[2]PT. Timah Tbk, Jl. Jenderal Sudirman No. 51 Pangkal Pinang, 33121, Bangka Belitung, Indonesia
[3]Department of Chemical Engineering, Faculty of Engineering, Universitas Gadjah Mada, Jalan Grafika No 2, Yogyakarta, 55281, Indonesia
[4]Unconventional Geo-Resources Research Center, Faculty of Engineering, UGM, Jl. Grafika No.2, Universitas Gadjah Mada, Yogyakarta, 55281, Indonesia

Abstract. Indonesia has been one of the world's primary source of tin since the early of 19th century. Bangka island has the largest tin abundant with a side product is zircon sand ($ZrSiO_4$). The existence of zircon ($ZrSiO_4$) is mostly associated with some of the valuable oxide compounds (VOC) and rare earth oxides (REO). The zirconia powders were synthesized from the zircon sand of PT. Timah Tbk by caustic fusion method followed by sol-gel method. The raw material zircon sand and as-synthesized zirconia were characterized through x-ray fluorescence (XRF), x-ray diffraction (XRD), surface area analysis and porositymeter, thermogravimetric and differential scanning calorimetry analysis (TG-DSC), fourier transform infra-red (FTIR) and scanning electron microscopy (SEM) techniques. The results show that zircon sand from PT Timah Tbk contains some of VOCs, such as $ZrSiO_4$, ZrO_2, HfO_2, SiO_2, Al_2O_3, TiO_2, Fe_2O_3 and some REOs, such as La_2O3, Y_2O_3, Nb_2O_5. The fusion temperatures varied from 600 to 800 ºC which resulted in an increase of the purity of ZrO_2 to 76% based on the XRF analysis. The surface area analysis and porositymeter results showed the significant change in specific surface area, pore size and pore volume of as-synthesized zirconia. The specific surface area increased dramatically from 0.28 m^2/g to 173.97, 125.18, and 102.14 m^2/g, at fusion temperatures of 600, 700, and 800 °C, respectively. The average particle size of as-synthesized zirconia showed the significant change from 21.31µm to 34.48 nm. The results of this work open new opportunities for the development of zirconia-based nanoparticles from the side product of tin mining.

1 Introduction

Indonesia is endowed with enormous mineral raw materials that have a wide range of applications, but unfortunately, they are either neglected or under-tapped. One example of such materials is the local zircon sand. Several years ago, it was considered as a waste because the benefit and economic value was not known at that time [1]. Predictions of zircon sands in Indonesia to 2023 show a positive trend. The production of zircon sand in Indonesia is 4% of global zircon production. Global needs in zircon sand grow rapidly makes its price increase drastically [2]. Zircon sand occurs in many parts of Indonesia such as Bangka-Belitung island where it is associated as a side product of tin mining. However, it contains several undesired impurities and a complex process is required. If a purified zircon powder can be achieved, a series of functional materials can be derived, including zirconia nanoparticles. Zirconia nanoparticles may further be modified its physicochemical properties to high performance engineering material, such as electronic devices, biomedical applications, polycrystal ceramic, foundry, catalyst, gas sensor, refractories, pigments, and as abrasives [3,4].

Many researches have been conducted to explore the utilization of zircon sand. The method used to produce zirconia powder depends on the desired characteristic of product, such as high-quality nanometer-sized powder. Several methods have been used for zircon decomposition, such as thermal dissociation by plasma [5], sintering with a source of alkali earth oxides [6], mechanochemical treatment followed by acid attack [7], and caustic fusion [4]. Among these, caustic fusion processes have been proposed to be an effective method for the decomposition of zircon sand. A higher purity zircon with good physicochemical properties needs to be developed.

Musyarofah, et al synthesized zirconia from Indonesian zircon sand by using a bottom-up method via caustic fusion and co-precipitation processes followed by calcination. Polymorph zirconia (ZrO_2-amorphous, tetragonal, and monoclinic) were successfully produced with the crystallite size estimated from X-ray diffraction (XRD) data analysis were 40, 31, and 61 nm, respectively [3]. Subuki, et al synthesized monoclinic zirconia

powders from the zircon sand by caustic fusion method at calcination temperatures between 500-800 °C. The results showed that the obtained powder had almost similar characteristics to that of the commercial powder. He also investigated the influence on ratio of $NaOH/ZrSiO_4$ in caustic fusion method for zircon sand. It was found that caustic fusion method followed by thermal treatment produced a higher yield of zirconium with lower impurities. The optimum ratio of $NaOH/ZrSiO_4$ of 1.2 produced lowest silicon impurity of 2.11wt% and high yield of zirconium at 71.40wt% [4]. Septawendar prepared zirconia nanoparticles from local zircon by a modified sodium carbonate sintering method, followed by leaching, slow hydrolysis, and calcination at a low temperature. It was resulted zirconia in 83.19% of purity, with particles less than 40 nm and surface area of 46.990 m^2/g [8]. Pusporini, et al reported the refinery process of zircon sand into several zirconium mineral products, including zircon opacifier, $ZrOCl_2$, $Zr(SO_4)_2$, and ZrO_2. The process began with physical separation continued by chemical purification [9].

Herein, the synthesis followed by physical and chemical characterization of zirconia nanoparticles derived from zircon sand ex-tin mining was conducted.

2 Experimental method

2.1 Materials

Zircon sand from Unit Metalurgi PT. Timah Tbk company in Muntok, Bangka Belitung Province is used as raw material. The Analytical Reagent (AR) grade chemicals of NaOH (99%), HCl (37%), Ammonia (25%) were used. Deionized water was used in all experiments.

2.2 Synthesis of zirconia powder

The zirconia nanoparticle was synthesized by using the caustic fusion method followed by sol-gel synthesis. NaOH was weighed at 30 g and zircon at 33 g [10]. The mixture of zircon sand and NaOH was placed on a zirconium crucible as a container. The temperature of caustic fusion process was varied at 600, 700 and 800 ℃ for 3 h. Caustic fusion products were left for 24 h in the muffle furnace, whereas the furnace turned off to ensure the solid product had reached ambient temperature. Caustic fusion products were dissolved by using deionized water at 80 °C. The water leaching residue was separated by using vacuum filtration and dried in an oven at 100 °C. Subsequently, the acid leaching method was used to produce $ZrOCl_2$ by dissolving the mixture in 100 mL of 3 M HCl solution. The process was conducted at 60 °C for 60 min. The $ZrOCl_2$ produced was titrated with NH_4OH 1 M until the pH of the solution becomes 9 to obtain the wet gel of $Zr(OH)_4$. The wet gel formed was allowed aging for overnight. Then, it was filtered and washed with deionized water until neutral. The neutralized gel was dried overnight in an oven at 100 ℃ and calcined at 700 ℃ for 5 h. The obtained zirconia nanoparticle samples with various temperatures of the caustic fusion process (600, 700 and 800 ℃) were denominated ZrNP1, ZrNP2, and ZrNP3, respectively.

2.3 Characterization

Characterization were conducted to evaluate the physicochemical properties of the synthesized zirconia powders. The morphology of the raw material was observed by field emission scanning electron microscopy (FESEM) JIB-4610F equipped with a Schottky electron gun, as well as a new focused ion beam (FIB) column capable of large current processing (maximum ion current of 90 nA) installed into one chamber. X-ray fluorescence (XRF) S2 PUMA-Bruker was used to determine the chemical composition in the zircon sand as raw material and after treatments. The thermal behavior of the powders was analyzed by thermogravimetric and differential scanning calorimetry analysis (TG-DSC) LINSEIS STA 1600. The powders were then heated from room temperature to 1000 °C at a heating rate of 10 °C/min in a flowing nitrogen atmosphere. X-ray diffractometer (XRD) Rigaku was used at a scan speed of 2°C/min over a scan range between 10°-90° to examine the phase that is present in the powder. Surface area analyzer and porositymeter Micromeritics TriStar II 3020 was used to measure the specific surface area, pore size, and pore volume of the samples through nitrogen adsorption-desorption isotherms, performing at 77.3 K on a liquid nitrogen apparatus after degassing the sample at 350 ℃ for 4 h. The surface structure of the powders was assessed using fourier transform infrared spectroscopy (FTIR) FTIR Bruker Tensor II with ATR attached to an automatic data acquisition center. Background spectra were acquired at 4 cm^{-1} resolutions, over the range of 500 – 4000 cm^{-1}.

3 Result and discussion

The FESEM micrograph of raw material shows angular blocky shape as shown in Figure 1. It indicates that raw material zircon sand has prismatic and pyramidal morphology [11].

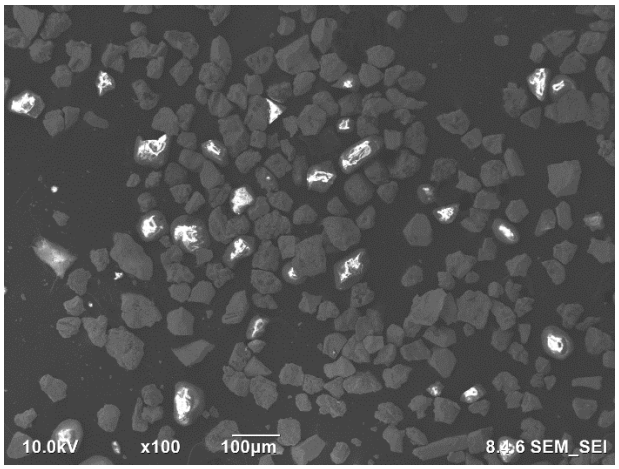

Fig. 1. FESEM image of raw material.

The XRF analysis of the raw material found the zirconia content is 50.62% as shown in Table 1. The impurities are still existed i.e SiO_2, SnO_2, TiO_2, Al_2O_3, Fe_2O_3, HfO_2, La_2O_3, Y_2O_3, MoO_3, and others. Higher impurities reduce the efficiency of zirconia synthesised from zircon sand. Thus, several steps are needed to be developed to remove these impurities and increase the zirconium content.

Table 1. Chemical composition of raw material (zircon sand) and zirconia nanoparticle samples (ZrNPs).

Compound	Raw material (%)	ZrNP1 (%)	ZrNP2 (%)	ZrNP3 (%)
Al_2O_3	2.10	2.10	1.10	2.00
Fe_2O_3	1.30	1.20	1.30	1.20
HfO_2	1.60	1.50	1.60	1.80
La_2O_3	0.70	1.10	1.10	1.10
MoO_3	0.30	0.30	0.40	0.50
Nb_2O_5	0.10	0.10	0.00	0.00
SiO_2	21.30	14.70	14.10	9.00
SnO_2	16.60	10.30	8.40	6.00
TiO_2	2.50	1.40	1.50	1.40
Y_2O_3	0.40	0.50	0.60	0.60
ZrO_2	50.60	66.40	69.50	76.00

The zirconia nanoparticles were synthesized using the common approach of sol-gel process using zircon sand obtained from tin plant. The chemical composition of the nano particle is depicted in Table 1. The major element in ZrNPs which is zirconium showed an increment in composition from 50.60 to 76% after treatment. The highest zirconium composition obtained was recorded at 76% with caustic fusion temperature of 800 °C. The silicon composition decreased from 21.30 to 9% after the fusion and thermal treatment. The caustic fusion temperature of 800 °C is deemed as the optimum ratio of $NaOH/ZrSiO_4$ because it resulted high yield of zirconium with lowest silicon composition. It indicated that higher temperature during caustic fusion process enhance sodium hydroxide to break the chemical bond between ZrO_2 and SiO_2 and form alkali zirconium compound. Subsequently, the leaching process will remove excess NaOH, unreacted zircon and sodium silicate. The reactions involved are as follows:

$$ZrSiO_4 + 6NaOH \rightarrow Na_2ZrO_3 + Na_4SiO_4 + 3H_2O$$
$$Na_2ZrO_3 + 2H_2O \rightarrow ZrO(OH)_2 + 2NaOH$$
$$Na_2ZrO_3 + 4HCl \rightarrow ZrOCl_2 + 2NaCl + 2H_2O$$

The zirconium hydroxide obtained using sol-gel route through pH control of the precursor solution, $ZrOCl_2$. Slow addition of NH_4OH 1 M until the pH of the solution becomes 9 to obtain the wet gel of $ZrO(OH)_2$.

$$ZrOCl_2 + 2NH_4OH \rightarrow Zr(OH)_4 + 2NH_4Cl$$

$$Zr(OH)_4 \rightarrow ZrO(OH)_2 + H_2O$$

Fig. 2 shows the TG-DSC curves of the ZrNP as-synthesized. After heating the sample from room temperature up to 1000 °C, the total weight loss was 24.68%. This amount of weight loss corresponds to the evolution of water vapor throughout the decomposition reaction. Zirconium hydroxide converts to zirconia by losing its water during the heat treatment by this reaction.

$$ZrO(OH)_2 \rightarrow ZrO_2 + 2H_2O$$

The DSC curve also shows exothermic peaks due to crystallization of tetragonal ZrO_2 from amorphous $ZrO(OH)_2$ at 874 °C. These results are in agreement with the XRD results.

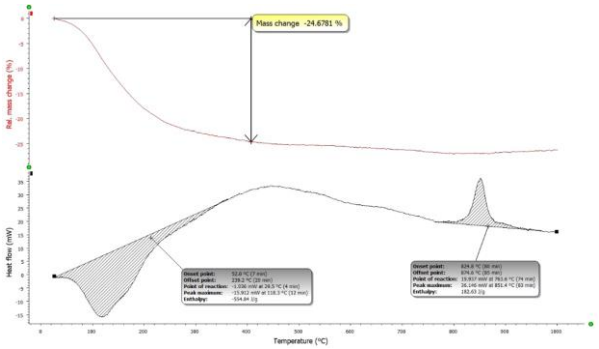

Fig. 2. TG and DSC curves of ZrNP-as synthesized zirconia nanoparticles.

XRD pattern for raw material shows predominant crystalline phase of zirconium silicate ($ZrSiO_4$). The highest peak was detected at 2Θ = 28.1° (111) (JCPDS card no.78–1807) which is indicative to monoclinic phases of crystalline zircon as shown in Fig. 3. A small trace of quartz and casserite are also observed. This data supports the composition analysis by XRF that zirconium and silicon as the main and second elements in raw material.

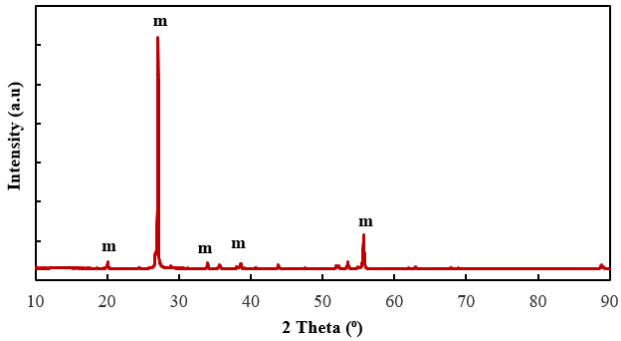

Fig. 3. XRD pattern of zircon sand raw material.

Fig. 4 shows XRD patterns of the ZrNP samples that were prepared at different temperatures in the caustic fusion process, which ranged from 600 to 800 °C. The XRD peaks in pattern ZrNP1 and ZrNP2 shows broad peak at 2θ = 30.6 ° which indicates the formation of ZrO_2 crystallite according to Joint Committee on Powder Diffraction Standard (JCPDS). However, the intensity of these peaks increased when the caustic fusion temperature

was increased to 800 ºC. The XRD pattern of ZrNP3 shows tetragonal phases of zirconia 30.2° (101), 50.2° (112) and 60.2° (211) (JCPDS card 79-2769) [10,12].

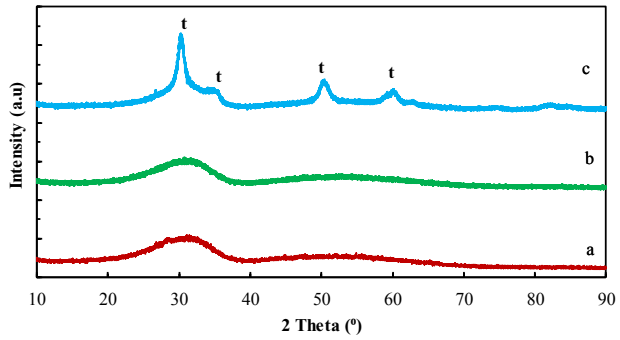

Fig. 4. XRD pattern of zirconia nanoparticles (a) ZrNP1, (b) ZrNP2, (c) ZrNP3.

We further examined the specific surface area (SBET), average pore size and total pore volume of the raw material zircon sand, ZrNP1, ZrNP2, and ZrNP3 samples. As can be seen in Table 2 that the specific surface area of all the ZrNP samples increased dramatically, whereas the raw material zircon sand was observed to have surface area of only 0.28 m^2/g. The rise in caustic fusion temperatures affected the specific surface area which the highest surface area was obtained at caustic fusion temperature of 600 °C. This is probably because the zirconia was defined as amorphous zirconia due to its high surface area. Sample ZrNP1 showed the highest specific surface area of 173.97 m^2/g compared to samples ZrNP2 and ZrNP3.

Table 2. Surface area analysis and porosity analysis results.

Sample	Specific surface area (m^2/g)	Pore size (nm)	Pore volume (cm^3/g)	Average nanoparticle size (nm)
Raw material	0.28	97.25	0.01	21,311.41
ZrNP1	173.97	2.82	0.12	34.49
ZrNP2	125.18	2.88	0.09	47.93
ZrNP3	102.14	4.76	0.12	58.74

Fig. 5 showed that all the ZrNP samples exhibit a type IV N_2 adsorption and desorption isotherms with a notable H4 type hysteresis loop due to the presence of mesopores. Sample ZrNP1 showed higher adsorption quantity in the range of ~ 26.7-79.3 cm^3/g compared to that of ZrNP2 and ZrNP3. This confirms the previous results whereas sample ZrNP1 has the highest specific surface area. The average particle size changed dramatically from 21.31 µm to be in the nanostructure range for ZrNP1, ZrNP2 and ZrNP3 samples of 34.49, 47.93 and 58.74 nm, respectively.

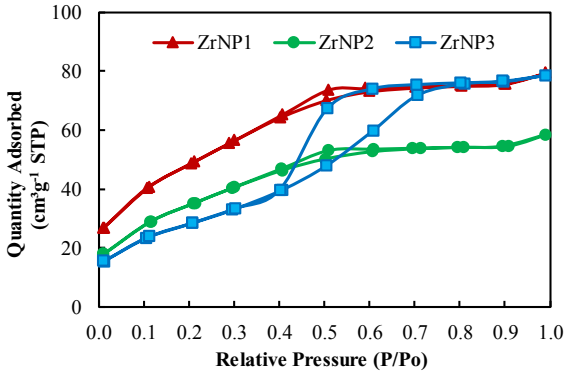

Fig. 5. N_2 adsorption and desorption isotherms of zirconia nanoparticles (a) ZrNP1, (b) ZrNP2, (c) ZrNP3

The presence of zirconia functional groups in the samples before and after sol-gel synthesis were analyzed by FTIR. As shown in Fig. 6, the adsorption band observed around 490-745 cm^{-1} in all samples correspond to the stretching vibration of Zr-O in the ZrO_2 phase [13,14]. The intensity peaks around 600 cm^{-1} which were linked to bending vibration of SiO_2 [11] is less observed in ZrNP as-synthesized because the effect of decomposition of raw material, $ZrSiO_4$. ZrNP as-synthesized shows the significant absorption bands in the range of 1250-1650 cm^{-1} correspond to bending vibration of Zr-OH and H-O-H vibrations of scissor type protons of water physically absorbed [7]. The broad peaks in the region of 3200 to 3800 cm^{-1} also observed in ZrNP as-synthesized is due to stretching vibration -OH group of water molecules absorbed by ZrO_2 nanoparticles [11].

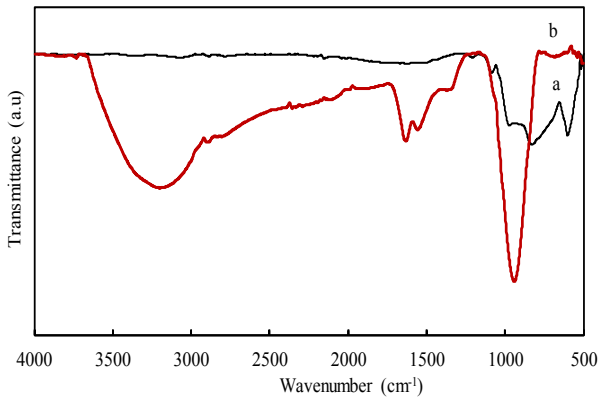

Fig. 6. FTIR spectra of (a) zircon sand raw material and (b) as-synthesized zirconia nanoparticles

4 Conclusion

In summary, we have synthesized zirconia nanoparticles through caustic fusion process followed by the sol-gel synthesis using zircon sand from side product of tin mining. The characterization results show that the increase in caustic fusion temperature gave significant effect on the zirconia content, phase formation, specific surface area, and particle size. The structure of ZrNP changed from monoclinic to tetragonal and the size decreased significantly from µm to nm. The results from

this work open future works for the development of zirconia nanoparticle from the zircon sand.

The authors would like to acknowledge Japan-ASEAN Science, Technology and Innovation Platform (JASTIP), National Research and Innovation Agency (BRIN), and PT. Timah Tbk for the research funding. The authors also acknowledge the facilities, scientific and technical support from Advanced Characterization Laboratories Serpong, National Research and Innovation Institute through E- Layanan Sains, Badan Riset dan Inovasi Nasional.

References

1. Samin, H. Poernomo, K. Rozana, and Suyanti, AIP Conf. Proc. **2296**, (2020)
2. G. Prameswara, I. Trisnawati, H. Poernomo, P. Mulyono, A. Prasetya, and H. T. B. M. Petrus, Mining, Metall. Explor. **37**, 1297 (2020)
3. Musyarofah, N. D. Lestari, R. Nurlaila, N. F. Muwwaqor, Triwikantoro, and S. Pratapa, Ceram. Int. **45**, 6639 (2019)
4. I. Subuki, ASM Sci. J. **17**, 1 (2022)
5. A. Smorokov, A. Kantaev, D. Bryankin, A. Miklashevich, M. Kamarou, and V. Romanovski, Miner. Eng. **189**, 107909 (2022)
6. A. M. Abdelkader, A. Daher, and E. El-Kashef, J. Alloys Compd. **460**, 577 (2008)
7. T. Dallali Isfahani, J. Javadpour, A. Khavandi, R. Dinnebier, H. R. Rezaie, and M. Goodarzi, Int. J. Refract. Met. Hard Mater. **31**, 21 (2012)
8. R. Septawendar, A. Nuruddin, S. Sutardi, E. Maryani, L. A. T. W. Asri, and B. S. Purwasasmita, J. Aust. Ceram. Soc. **54**, 643 (2018)
9. N. D. Pusporini, Suyanti, R. A. Amiliana, and H. Poernomo, J. Phys. Conf. Ser. **1436**, (2020)
10. I. Subuki, M. F. Mohsin, M. H. Ismail, and F. S. M. Fadzil, Indones. J. Chem. **20**, 782 (2020)
11. I. Otoijamun, M. Kigozi, A. R. Adetunji, and P. A. Onwualu, Minerals **11**, (2021)
12. N. B. Nayak and B. B. Nayak, Sci. Rep. **6**, 1 (2016)
13. S. Mallakpour and A. Nezamzadeh Ezhieh, Polym. - Plast. Technol. Eng. **56**, 1136 (2017)
14. D. C. Escalante-Gutiérrez, E. Ordóñez-Regil, J. Ortíz-Landeros, and M. G. Almazán-Torres, Radiochim. Acta **108**, 847 (2020)